

Click-connected 2-(hydroxyimino)aldehydes for the design of UV-responsive functional molecules

Francesca D'Acunzo^{*[a]}, Linda Carbonaro^[b], Antonella Dalla Cort^[a, b], Antonio Di Sabato^[a, b], Dario Filippini^[b], Francesca Leonelli^[b], Laura Mancini^[b] and Patrizia Gentili^{*[a, b]}

[a] Dr. F. D'Acunzo, Prof. A. Dalla Cort, Dr. A. Di Sabato, Prof. P. Gentili
Istituto per i Sistemi Biologici, Sezione Meccanismi di Reazione
Consiglio Nazionale delle Ricerche
c/o Dipartimento di Chimica, Sapienza Università di Roma
P.le A. Moro 5, 00185 Roma, Italy
E-mail: francesca.dacunzo@cnr.it, patrizia.gentili@uniroma1.it

[b] Dr. L. Carbonaro, Prof. A. Dalla Cort, Dr. A. Di Sabato, Dr. D. Filippini, Prof. F. Leonelli, Dr. L. Mancini, Prof. P. Gentili
Dipartimento di Chimica
Sapienza Università di Roma
P.le A. Moro 5, 00185 Roma, Italy

Supporting information for this article is given via a link at the end of the document

Abstract: We use click chemistry to functionalize simple lipophilic and water-soluble molecules, a complex PEGylated phospholipid (DSPE-PEG2000), and two benzylic substrates with the 2-(hydroxyimino)aldehyde (HIA) group. To this end, we synthesize two terminal alkynes bearing the HIA moiety and we couple them to different azides through copper(I)-catalyzed azide alkyne cycloaddition (CuAAC). Norrish-Yang photoisomerization ($\lambda = 365$ nm, LED source) is successfully obtained, with no interference by the triazole linker, except when the forbidden $n-\pi^*$ carbonyl transition is screened by a remote substituent such as salicylaldehyde. UV-Vis spectrometry suggests a specific interaction of HIAs with Cu(II), whereas no such evidence is found with Cu(I). We thereby show that the CuAAC methodology can be used successfully to obtain HIA-based UV-responsive hydrophilic or lipophilic ligands, phospholipidic components for the construction of liposomes, and macrocycle precursors.

The 2-(hydroxyimino)aldehyde (HIA) group exhibits a rich photochemistry (Figure 1) encompassing *E/Z* configurational isomerism of the oxime group and Norrish-Yang rearrangement of the carbonyl group.^[1] The latter results in the formation of the cyclobutanol oxime (CBO) structure with the hydroxyl group and the substituent on the adjacent position on either side of the ring.^[2] The stereoselectivity of this process is determined by the stereoelectronic requirements of ring closure and may be influenced by other factors, such as solvent polarity and hydrogen bonding.^[3] The Norrish-Yang photochemical reactions were observed by Cerfontain on a series of 2-oxo-oximes, their ethers and esters, in a number of papers published between the late 70's and early 90's (see, for instance^[4-7] *et seq*). The photoisomerization aspect of this body of work received limited attention, whereas the photolysis of oxime esters to iminyl radicals has been investigated for the initiation of radical polymerizations.^[8] However, the interest in practical aspects of

photochemistry is increasing as convenient LED sources become available across the UV-Vis spectrum, also allowing for flow photochemistry setups.^[9-11] Therefore, the photoreactions of oxime and carbonyl compounds have been attracting a renewed attention in contemporary applications, such as the manipulation of soft materials properties^[12] and synthetic photochemistry and photocatalysis.^[13] For instance, we recently showed that the photochemistry of the HIA group has a remarkably large impact on the physico-chemical behavior of aqueous solutions of copolymers of OEGMA and an HIA-functionalized methacrylate.^[14] Applications of the HIA to CBO photoisomerization can be envisaged in metal ligation and sensors.^[15,16] Furthermore, the cyclobutanol motif is of interest in organic synthesis as a prochiral unit,^[17] it is present in natural products^[18] and has been used as an intermediate in the total synthesis of some sesterpenoids.^[19] In a recent report, the Cu-catalyzed reductive coupling of cyclobutanone oxime ester with

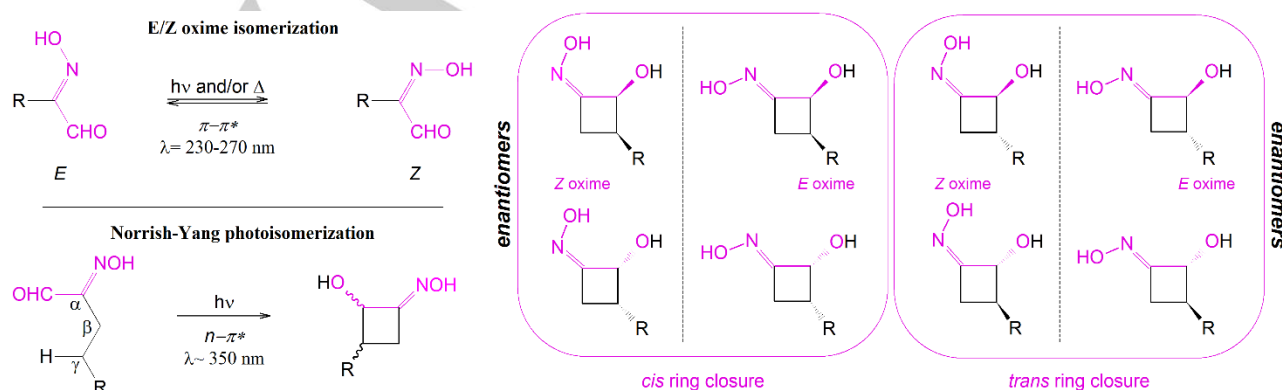


Figure 1. Main reactions in the photochemistry of HIAs and stereochemistry of CBO formation by *cis* or *trans* ring closure

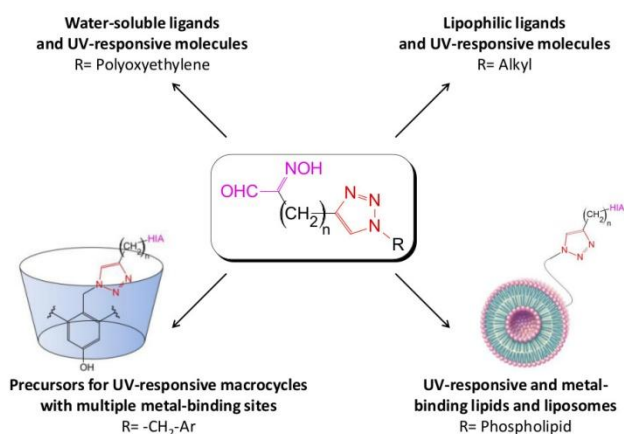


Figure 2. Prospective uses of the structures obtained in this work.

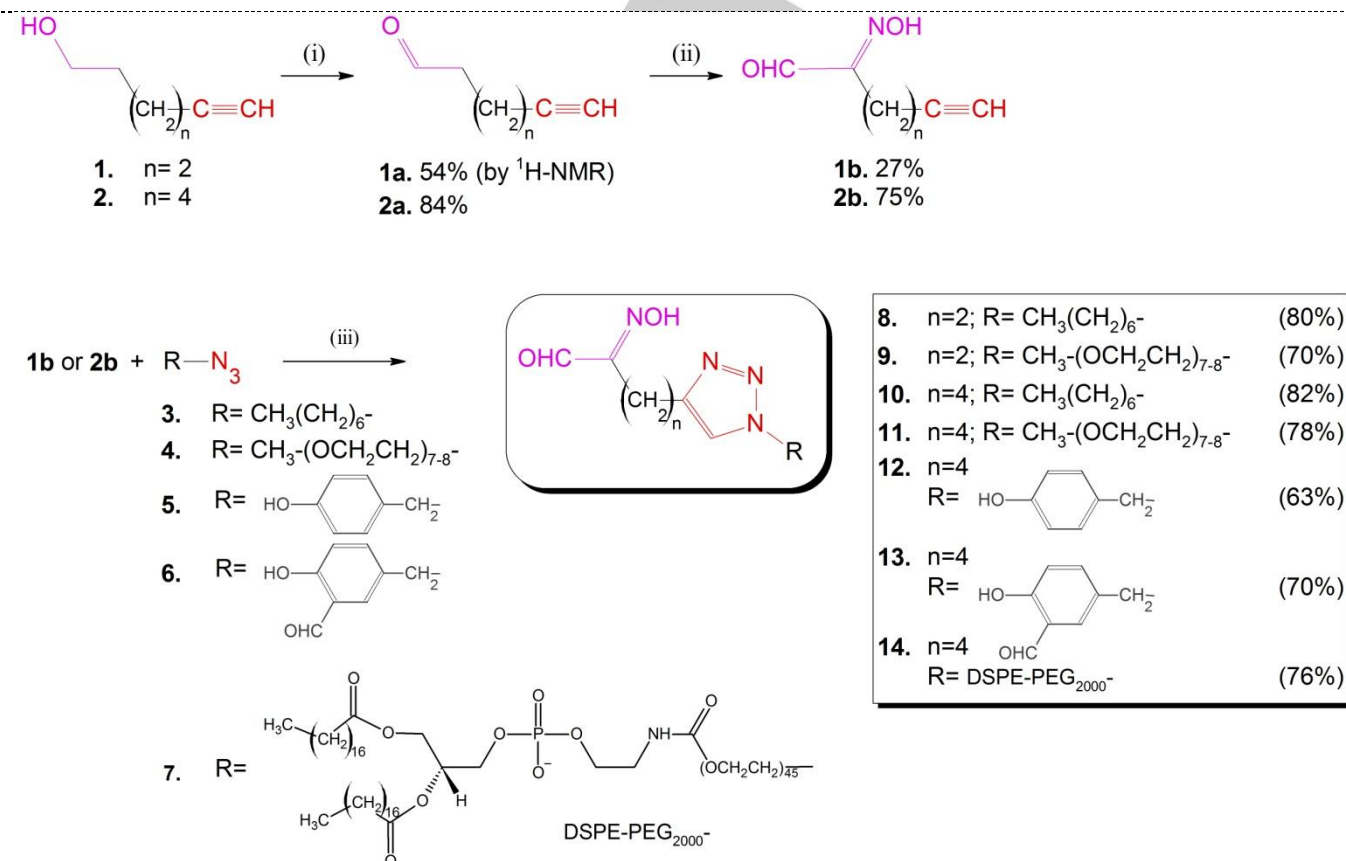
terminal alkynes afforded a route to the direct alkylation of remote unfunctionalized sp^3 carbon.^[20] Several examples are provided in the literature for the metal-catalyzed synthesis of cyclobutane, cyclobutene and cyclobutanol derivatives through enantioselective [2+2] cycloaddition reactions^[21] or cyclizations involving γ -activated precursors.^[22–24] In contrast, the Norrish-Yang cyclization of carbonyls involves a non-activated, aliphatic C-H bond in γ -position. HIAs have been obtained in good yields in our group by α -oximation of aliphatic or benzylic aldehydes.

However, aldehyde precursors may be of limited stability due to spontaneous condensation or oxidation. Furthermore, the yield of the α -oximation reaction depends on the bulk and nature of the neighboring group. In fact, in our previous investigations the yields of different HIAs range from 45% to 90%.^[2,25] The reaction failed altogether when we attempted it on $m\text{PEG}_{300}$ - $\text{O}(\text{CH}_2)_5\text{CHO}$. Therefore, it may prove sensible to graft the pre-formed HIA group onto the desired platform instead of dealing with the compound-specific outcome of the α -oximation reaction. The goal is to obtain stimuli-responsive functional molecules, i.e. structures designed to serve specific tasks. In this work, we use click chemistry to functionalize diverse precursors with the HIA group in view of exploring their potential as UV-responsive moieties in lipophilic or water-soluble molecules, liposomes and macrocycles (Figure 2). Since the use of click chemistry brings about the introduction of a triazole ring as linker between the HIA and the rest of the molecule, we assess the influence of the linker on the Norrish-Yang photoisomerization to CBO. In the context of CuAAC we also look into the interaction of HIAs with Cu(I) and Cu(II) ions.

Results and Discussion

We synthesized two HIA-functionalized terminal alkynes for the standard copper-catalyzed azide-alkyne 1,4-Huisgen cycloaddition (CuAAC; Scheme 1, top).

Scheme 1. Synthesis of CuAAC-ready HIA derivatives and their reaction with different azides



Top: Synthesis of HIAs with a terminal triple bond for CuAAC (**1b** and **2b**). Bottom: HIAs **1b** and **2b** are reacted with azides **3-7** through CuAAC. Reaction conditions: (i) $\text{SO}_3\text{-Py}$ (3 equiv), Et_3N (4 equiv), DMSO , CH_2Cl_2 , 0°C 1h then RT 3h; (ii) $p\text{-TsOH}$ (0.2 equiv), pyrrolidine (0.2 equiv), H_2O (2 equiv), NaNO_2 (1 equiv), FeCl_3 (1 equiv), DMF ; (iii) 2,6-lutidine (2 equiv), $(i\text{-Pr})_2\text{EtN}$ (2 equiv), CuI (0.1 equiv), CH_3CN , RT, 3h. Given yields are after purification on silica gel column.

The two HIA-alkynes **1b** and **2b** only differ by the length of the carbon chain separating the two functional groups. Azides with alkyl (**3**), oligo(ethylene glycol) (**4**), benzyl (**5**, **6**) and PEGylated phospholipid residues were also synthesized in good to excellent yields. We used commercial 5-hexyn-1-ol **1**, whereas we chose to obtain 7-octyn-1-ol **2**, also available commercially, by base-catalyzed isomerization ("Acetylene zipper" reaction)^[26] of 3-octyn-1-ol in very good yield (79%) after purification. The two-step synthesis of HIA **2b** from **2** proceeded smoothly to an overall 63% yield after purification (Scheme 1). The 75% yield of the α -oximation step of **2a** is in keeping with the yields of other unhindered HIAs.^[2] Intermediate **1a**, on the other hand, could not be isolated from the petroleum ether used in the column chromatography purification, even after repeated distillation, as already reported by other Authors.^[27] Therefore, the α -oximation of **1a** was conducted in the presence of 27% residual hexanes (estimated from ¹H-NMR, see Supporting Information), and this may be one of the factors leading to the low yield of **1b** (27%), as this reaction is solvent-sensitive.^[25] To link **1b** and **2b** to molecules of different nature we, then, utilized CuAAC with Cu(I) and no reductant in a degassed environment (Scheme 1, bottom). The click reaction worked smoothly in 3-5h on all azides **3-7** and no significant differences are observed between alkyne **1b** and **2b**, with 80% and 82% yield of products **8** and **10**; 70% and 78% of **9** and **11**, respectively. We thereby conclude that even though the neighboring HIA may potentially interact with copper ions, it does not interfere with the CuAAC reaction in the above conditions. We also tested the popular Cu(II)/reductant catalyzed CuAAC on azide **3** and 5-hexyn-1-ol (Supporting Information) and we compared its outcome in the presence of a stoichiometric amount of 2-(hydroxyimino)-3-octyltridecanal (HIOTD, Fig. 3a), a simple model HIA with no other substituents.^[2] This way, we were able to check if the HIA group inhibits the Cu(II)/reductant catalytic system. The reaction was carried out in DMSO to ensure full solubility of HIOTD. The reaction is slower compared to the click reactions in Scheme 1 even in the absence of HIOTD. After 48h, we obtained 70% yield of the triazole product, whereas the yield dropped to 15% when Cu(II) was added to the HIOTD-containing mixture. A somewhat better outcome (30% yield) resulted from adding pre-mixed copper-ascorbic acid to the reaction mixture, thus reducing Cu(II) prior to coming into contact with the HIA. To gain some insight into the interaction between HIA and copper ions, we looked into the effect of Cu(I) and Cu(II) addition to the UV-Vis spectrum of HIOTD (Figure 3a, b). We do not observe any effect of HIOTD on the UV-Vis spectrum up to 1:3 CuI/HIOTD in acetonitrile (Figure 3a). Upon addition of Cu(OAc)₂ to HIOTD (Figure 3b), a hyperchromic effect and the suppression of the typical Cu(II) band at $\lambda=670$ nm is observed, along with the appearance of a new band at $\lambda=413$ nm. In the case of chromatographically purified HIA **11** we observed an unexpected broad band extending just over 400 nm and no free Cu(II) band ($\lambda=600-700$ nm). As a working hypothesis based on the HIOTD-Cu(II) spectra in Figure 3b, we surmised that this absorption results from HIA **11**-Cu(II) interaction and we attempted copper removal through treatment with an EDTA solution at pH 7.6-7.7. We avoided higher pH to limit deprotonation of the HIA moiety (pK_a of HIAs range 7.8-9), which may lead to HIA decomposition.^[2] The aqueous EDTA extracts exhibited a pale blue color confirming extraction of Cu(II) (Supporting Information), while the HIA **11** spectrum shows the characteristic

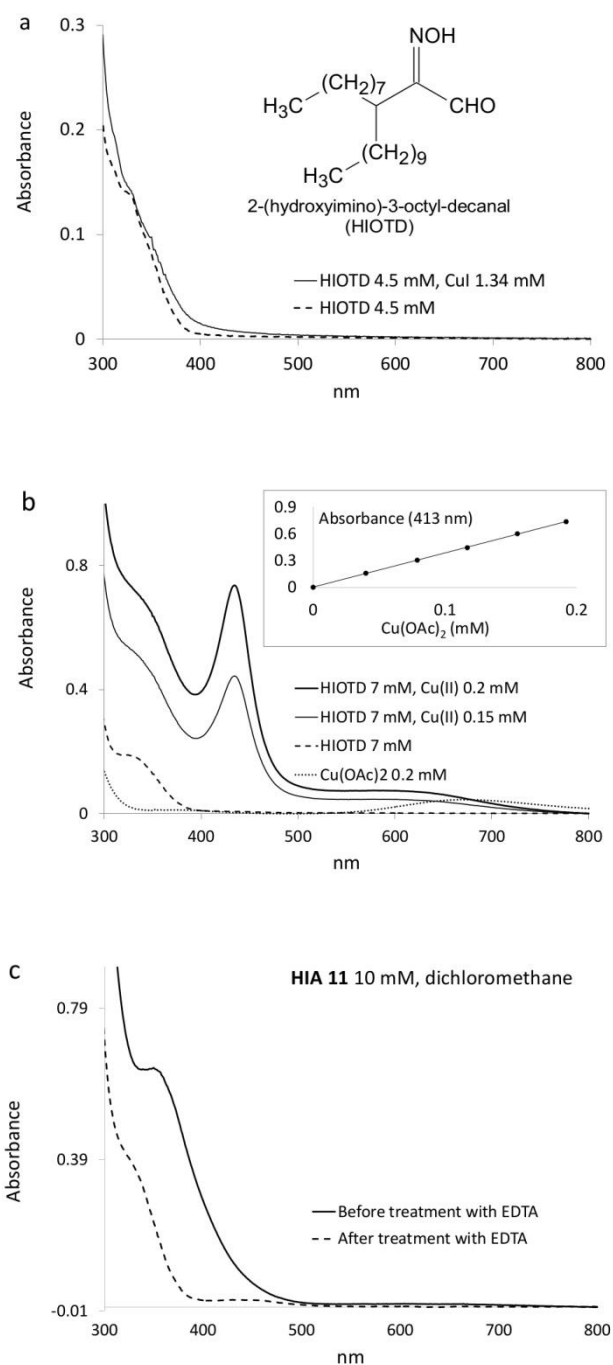
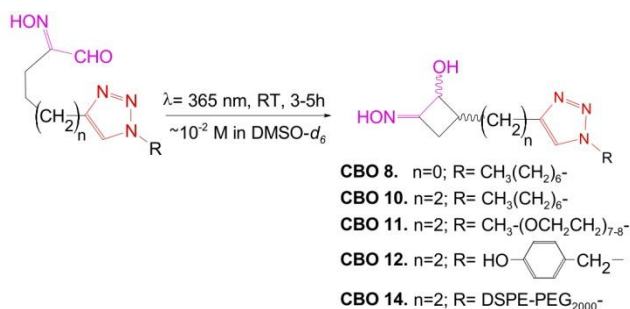


Figure 3. UV-Vis spectra of (a) the model HIA HIOTD in acetonitrile before and after addition of CuI; (b) HIOTD in acetonitrile with increasing concentrations of Cu(OAc)₂; (c) HIA **11** in dichloromethane before and after treatment with EDTA for copper removal. Inset in (b) shows a linear increase of absorbance at $\lambda=413$ nm as [Cu²⁺] is increased ($\epsilon=3840$ M⁻¹ cm⁻¹).

wavelength of the HIA $n-\pi^*$ transition, around 320 nm (Figure 3c).^[2] In short, these results suggest HIA ligation of Cu(II) and the observed inhibition of the Cu(II)/ascorbic acid CuAAC by HIOTD can, therefore be rationalized in terms of selective ligation of Cu(II) by the HIA group. In principle, the triazole residue in the HIA **11** may also participate in metal ion chelation.^[28] These preliminary data elicit a further dedicated study on HIAs and triazole-HIAs as ligands of different metal ions.

Scheme 2. Cyclobutanol oximes observed in this work by photoisomerization of HIAs



LED source assembly is described in the Supporting Information.

We have previously shown^[2] that HIAs isomerize to CBOs (Norrish-Yang reaction, Figure 1) when irradiated in a Rayonet photoreactor equipped with high pressure mercury lamps ($\lambda_{\text{max}}=350$ nm, about 100 nm broad). In the present study, we have used a 365 nm LED source (± 10 nm width at half height) to selectively induce the $n-\pi^*$ transition of the aldehyde group in HIAs **8**, **10-14** (Scheme 2).

The photo-isomerization was conducted directly in the NMR tube with DMSO- d_6 as solvent. Based on the disappearance of the CHO signals of HIAs in the ^1H NMR spectra (Figure 4), conversion to photoproducts was $>95\%$ in 3-5h only, whereas $>20\text{h}$ where necessary with the Rayonet photoreactor.^[2] NMR evidence (Figure 4 for ^1H NMR; Supporting Information for ^{13}C , DEPT135, $^1\text{H}-^1\text{H}$ COSY and HSQC experiments) for the formation of the Norrish-Yang product CBO is hereby provided, along the lines of our previous investigation on the photoinduced isomerization of a simple aliphatic HIA.^[2] The diagnostic signals in the ^1H NMR spectrum in DMSO- d_6 for CBOs are $>\text{C}=\text{N}-\text{OH}$ ($\delta \sim 10.5$ ppm, i.e. upfield by >2 ppm relative to the HIA oxime), and $>\text{CH}-\text{OH}$ signals ($\delta = 5.0-4.5$ ppm and $6.0-5.5$ ppm, respectively). These signals are easily detected in the NMR spectrum of photoproducts in Figure 4. The ^{13}C spectrum in the 35-0 ppm region is, alone, less informative than ^1H ; however, combined information from DEPT135 and HSQC allowed us to establish C-H connectivity. The formation of two major isomeric cyclic structures is highlighted by long-range correlations within two sets of analogous signals in the $^1\text{H}-^1\text{H}$ COSY45 experiments.

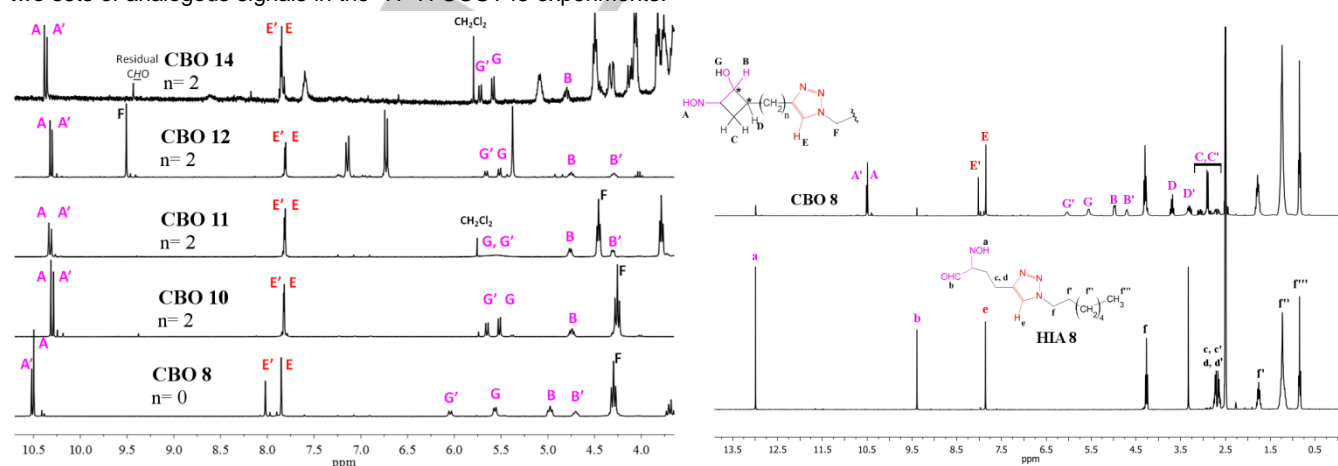


Figure 4. ^1H -NMR signals (DMSO- d_6 , δ , ppm) of CBOs **8**, **10**, **11**, **12** and **14** resulting from the Norrish-Yang photo-isomerization ($\lambda = 365$ nm) of the corresponding HIAs (Scheme 2). Left: expansion (11.0-4.0 ppm) of all CBO spectra. Right: Comparison of the full spectrum of CBO **8** with that of the parent HIA. Two sets of signals are observed with all CBOs due to the formation of a diastereomeric mixture.

In principle, up to four CBO diastereomers may be observed by NMR (Figure 1), resulting from the triazole substituent either *cis* or *trans* with respect to the $-\text{OH}$ attached to the cyclobutane ring and from *E/Z* isomerism of the oxime $>\text{C}=\text{N}-\text{OH}$. Only two major sets of NMR signals are present in the NMR spectra, instead. The two main $>\text{C}=\text{N}-\text{OH}$ signals (A/A') are detected in the 10.5-10.25 ppm range. When comparing CBO **8** and **10**, their chemical shift depends on the distance between the triazole and CBO rings. On the other hand, A/A' $\Delta\delta$ is only 0.02 ppm, regardless of the triazole position. A stronger effect is exerted on the $\text{CH}-\text{OH}$ signals by the distance between the triazole and cyclobutanol rings. Specifically, in CBOs **10**, **11**, **12** and **14**, in which the triazole and the CBO rings are spaced by two methylenes, the B/B' signals are separated by 0.4 ppm vs. 0.2 ppm in CBO **8**; E/E' 0.01 ppm vs. 0.15 ppm, and G/G' by 0.15 ppm vs. 0.5 ppm. In short, we observe a large effect of the vicinity of the triazole ring on the chemical shifts of the $\text{CH}-\text{OH}$ signals. Thereby, we find it reasonable to assume that the two main sets of signals correspond to the *cis* and *trans* isomers of the four-membered ring, rather than to the *E/Z* oxime isomers. It is worth noting, however, that a further pair of small peaks is observed in the 10.5-10.2 ppm region, which may account for the oxime configurational isomerism as well. (Figure 4). As for the diastereomeric ratio in CBO **8**, integration of A/A' , E/E' , G/G' and B/B' consistently indicates a slight excess of one ring closure (diastereomeric ratio, $dr = 65:35$). In CBOs **10** and **14**, dr is calculated from the intensities of the $>\text{CH}-\text{OH}$ peaks (G , G'), due to overlap of B' with other signals. In the spectrum of CBO **11** the G , G' peaks are, unlike oxime A and A' ,^[29] too broad to be observed due to rapid exchange. However, both $>\text{CH}-\text{OH}$ peaks (B , B') are clearly detected and the isomeric ratio is thus calculated. Negligible diastereoselection (dr close to 50:50) is thereby observed with CBOs **10**, **11**, **12** and **14**. This difference with respect to the dr of CBO **8** can be rationalized in terms of stereoelectronic requirements of the Norrish-Yang cyclization^[3] if we consider the distance between the triazole ring and the reacting center. In fact, in HIA **8** the triazole group is adjacent to the reacting C-H bond, whereas in HIA **10**, **11** and **12** it is separated by two methylene groups from the reacting γ -position (Scheme 2). HIA **13** did not yield any significant photoproduct, unlike HIA **12**, which also bears an aromatic R_1 group. This is due to the contribution of the salicylaldehyde moiety, which

exhibits a strong absorption band in the 370-300 nm region.^[30,31] This band, which smothers the forbidden $n-\pi^*$ HIA transition, is absent in HIA **12** (Supporting Information). We did attempt a scale-up of the HIA to CBO isomerization (60 mg of HIA **10** in 5 mL DMSO) with minor modifications of the illumination assembly, including the use of a more powerful LED source (see Supporting Information). HPLC monitoring of reaction progress showed the formation of one major product as the substrate was depleted by 90% in 24h. Upon routine workup (ethyl acetate/water partitioning and reduced pressure removal of solvent at room temperature), the product peak was no longer present in the HPLC trace and two different main peaks were detected, along with several impurities. ¹H-NMR analysis in DMSO-*d*₆ showed that the triazole linker was still present, whereas the CBO signals were no longer detected (Supporting Information). Therefore, so far we have not been able to isolate and fully characterize the single CBO diastereomers detected by NMR in the small scale reaction. Optimized reaction conditions and workup procedures are being sought to obtain CBOs for synthetic purposes.

Conclusions

CuAAC chemistry can be used successfully to anchor the 2-(hydroxyimino)aldehyde group to aliphatic, benzylic and PEGylated structures, including a complex phospholipid. To this end, we obtained two click chemistry-ready precursors in a two-step synthesis from commercial products. The HIA moiety retains the ability to undergo Norrish-Yang photoisomerization to cyclobutanol oxime also in the presence of a triazole ring as substituent. However, as the electronic transition involved in the Norrish-Yang is associated with a weak absorption, CBO fails to form when another functional group competes for the same wavelength, as is the case with the salicylaldehyde substituent. It should be noted that the Norrish-Yang reaction introduces two chiral centers in molecules with little or no chiral information. When the triazole ring is directly attached to the incipient cyclobutanol, ring closure exhibits some degree of diastereoselectivity, which fades as the triazole is further removed from the cyclization site. Reaction scale-up and isolation of CBOs are the next challenges towards their use in organic synthesis. Unequivocal identification of the observed CBO stereoisomers and, possibly, the elaboration of strategies to control ring closure stereochemistry are in order for synthetic purposes.

EXPERIMENTAL SECTION

Chemicals, equipment and detailed syntheses and product characterization are found in the Supporting Information.

Photochemical setup Supporting Information for Figures and detail. The photoreactor for NMR-scale experiments consists of a lab-made LED chip assembly equipped with a sample holder. The LED assembly is obtained by gluing a single LED chip (Nichia NVSU233A UV SMD-LED with PCB (10x10mm), $\lambda = 365$ nm, 1030 mW radiant flux, 3.75 V forward voltage from LUMITRONIX® LED-Technik GmbH) on an aluminum heat sink, using Fischer Elektronik heat-conducting adhesive WLK DK 4. The LED is powered with a constant current power supply (Meanwell LCM-40 Series, LUMITRONIX® LED-Technik GmbH). The light intensity delivered to the sample is determined by

chemical actinometry, using *o*-nitrobenzaldehyde (NBA) as the substrate.^[32]

UV-Vis spectrometry of 2-(hydroxyimino)-3-octyltridecanal / Cu ions

A solution of 2-(hydroxyimino)-3-octyltridecanal (HIOTD) in acetonitrile was placed in a 3 mL quartz cuvette. Spectra were recorded at 25°C after each addition of aliquots of either CuI or Cu(OAc)₂ in acetonitrile. CuI 8.9 mM, HIOTD 4.5 mM; CuI additions up to HIOTD/CuI = 3:1. Cu(OAc)₂ 4.6 mM, HIOTD 7 mM; Cu(OAc)₂ additions up to HIOTD/Cu(OAc)₂ = 30:1.

General procedure for Parikh-Doering oxidation: Compounds 1a and 2a.^[33] 1.0 mmol of alcohol, 7 mL CH₂Cl₂ and 0.54 mL (4.0 mmol) Et₃N are introduced in a flame-dried two-necked round bottomed flask equipped with a nitrogen inlet and magnetic stirring. The flask is chilled in an ice bath, then a solution of 0.48 g (3.0 mmol) SO₃-Pyridine complex in 3 mL DMSO is added. Stirring is continued at 0°C for 1h, then for 3h at room temperature. The following workup procedure is aimed at minimizing product loss and maximizing removal of DMSO from the reaction crude. The reaction mixture is diluted with CH₂Cl₂ or Et₂O and washed with a 1:1 (v/v) mixture of NH₄Cl (sat) and brine. Most of the CH₂Cl₂ (if used) is removed by rotary evaporation and the residue is taken up with Et₂O. The aqueous phase is extracted with fresh Et₂O to minimize product loss. The combined organic phases are washed again with the NH₄Cl/NaCl (sat), then with brine alone to remove as much DMSO as possible. After drying over anhydrous Na₂SO₄, the solvent is removed and the residue is purified by silica gel chromatography.

General procedure for α -oximation of aldehydes: Compounds 1b and 2b.^[25] In this order, 4 mL DMF, 36 μ L (2.0 mmol) H₂O, 17 μ L (0.20 mmol) pyrrolidine, 35 mg (0.20 mmol) *p*-toluenesulfonic acid and 1.0 mmol of aldehyde are introduced in a two-necked round bottom flask and magnetic stirring. Then 70 mg (1.0 mmol) of NaNO₂ are added, followed by 0.162 g (1.0 mmol) of FeCl₃ in small portions to avoid excessive heating. The reaction is continued for 4h at room temperature, the mixture is diluted with 20 mL EtOAc and 7 mL of a 1:1 (v/v) mixture of NH₄Cl (sat) and brine and stirred for 20 minutes at room temperature. The organic layer is set aside and the aqueous phase is extracted with 5 mL fresh EtOAc to minimize product loss. The pooled organic solutions are washed once more with 7 mL of NH₄Cl (sat)/brine mixture, then three times with brine. After drying over anhydrous Na₂SO₄, EtOAc is removed by rotary evaporation. The product is purified by silica gel chromatography.

General procedure for CuAAC reactions: Compounds 8-14.^[34] 1.0 mmol of alkyne and 1.0 mmol of azide are dissolved in 4 mL acetonitrile in a schlenk tube equipped with magnetic stirring. Then, 0.23 mL (0.21 g, 2.0 mmol) of 2,6-lutidine and 0.35 mL (0.26 g, 2.0 mmol) of diisopropylethylamine are added and the solution is degassed through three freeze-pump-thaw cycles under Argon. 19 mg of CuI (0.10 mmol) is added under Ar. The reaction was stirred for 3h at room temperature. Most of the CH₃CN is removed by rotary evaporation and the resulting residue is dissolved in 50 mL EtOAc. The organic phase is washed three times with 25 mL NH₄Cl_(sat), then with 25 mL HCl 0.1 M, and finally with 25 mL distilled water. After drying over anhydrous sodium sulfate, the solvent is evaporated and the residue is purified by column chromatography on silica gel. Removal of residual copper ions was achieved by washing a dichloromethane solution of the product several times with

EDTA 0.1M, previously adjusted at pH 7.6 (10:1 organic phase/EDTA solution).

Acknowledgements

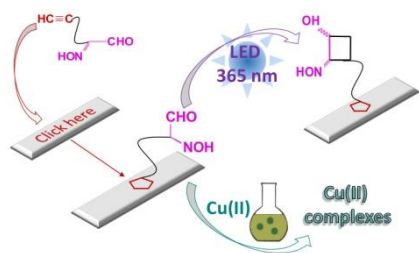
We thank Prof. Maria Elisa Crestoni of Dipartimento di Chimica e Tecnologie del Farmaco, Università di Roma "La Sapienza" for HRMS analyses. We also thank Dr. Carlo Sperilli of Università di Roma La Sapienza, Dipartimento di Chimica, and Mr. Enrico Rossi of CNR-ISB, for assembling the photochemical setup. Financial support by Sapienza Università di Roma, Research grant RM11816436CD375D 2018

Keywords: 2-(hydroxyimino)aldehyde • ciclobutanol oxime • click chemistry • photochemistry • LED

REFERENCES

- [1] C. Chen, *Org. Biomol. Chem.* **2016**, *14*, 8641–8647.
- [2] P. Gentili, M. Nardi, I. Antignano, P. Cambise, M. D'Abbramo, F. D'Acunzo, A. Pinna, E. Ussia, *Chem. - A Eur. J.* **2018**, *24*, 7683–7694.
- [3] J. N. Moorthy, P. Mal, *Tetrahedron Lett.* **2003**, *44*, 2493–2496.
- [4] P. Baas, H. Cerfontain, *J. Chem. Soc. Perkin Trans. 2* **1979**, 156–162.
- [5] P. Baas, H. Cerfontain, *J. Chem. Soc. Perkin Trans. 2* **1979**, 151–155.
- [6] P. Baas, H. Cerfontain, *J. Chem. Soc. Perkin Trans. 2* **1979**, 1653–1660.
- [7] T. S. V. Buys, H. Cerfontain, J. A. J. Geenevasen, F. Stunnenberg, *Recl. des Trav. Chim. des Pays-Bas* **1986**, *105*, 188–194.
- [8] D. E. Fast, A. Lauer, J. P. Menzel, A.-M. Kelterer, G. Gescheidt, C. Barner-Kowollik, *Macromolecules* **2017**, *50*, 1815–1823.
- [9] H. E. Bonfield, T. Knauber, F. Lévesque, E. G. Moschetta, F. Susanne, L. J. Edwards, *Nat. Commun.* **2020**, *11*, DOI 10.1038/s41467-019-13988-4.
- [10] F. Politano, G. Oksdath-Mansilla, *Org. Process Res. Dev.* **2018**, *22*, 1045–1062.
- [11] F. Secci, S. Porcu, A. Luridiana, A. Frongia, P. C. Ricci, *Org. Biomol. Chem.* **2020**, *18*, 3684–3689.
- [12] M. Nardi, F. D'Acunzo, M. Clemente, G. Proietti, P. Gentili, *Polym. Chem.* **2017**, *8*, 4233–4245.
- [13] J. A. Dantas, J. T. M. Correia, M. W. Paixão, A. G. Corrêa, *ChemPhotoChem* **2019**, *3*, 506–520.
- [14] F. D'Acunzo, S. De Santis, G. Masci, M. Nardi, P. Renzi, A. P. Sobolev, *Macromol. Chem. Phys.* **2019**, *220*, DOI 10.1002/macp.201900200.
- [15] N. Gerasimchuk, *Dalt. Trans.* **2019**, *48*, 7985–8013.
- [16] F. Ratsch, W. Schlundt, D. Albat, A. Zimmer, J.-M. Neudörfel, T. Netscher, H.-G. Schmalz, *Chem. - A Eur. J.* **2019**, *25*, 4941–4945.
- [17] J. Hatai, C. Hirschhäuser, J. Niemeyer, C. Schmuck, *ACS Appl. Mater. Interfaces* **2020**, *12*, 2107–2115.
- [18] B. Tang, R. S. Paton, *Org. Lett.* **2019**, *21*, 1243–1247.
- [19] Y. Chen, J. Zhao, S. Li, J. Xu, *Nat. Prod. Rep.* **2019**, *36*, 263–288.
- [20] Z. Li, R. O. Torres-Ochoa, Q. Wang, J. Zhu, *Nat. Commun.* **2020**, *11*, 403.
- [21] K. Ishihara, K. Nakano, *J. Am. Chem. Soc.* **2007**, *129*, 8930–8931.
- [22] D. Johnston, C. M. McCusker, D. J. Procter, *Tetrahedron Lett.* **1999**, *40*, 4913–4916.
- [23] T. Johnson, K.-L. Choo, M. Lautens, *Chem. - A Eur. J.* **2014**, *20*, 14194–14197.
- [24] A. Whyte, B. Mirabi, A. Torelli, L. Prieto, J. Bajohr, M. Lautens, *ACS Catal.* **2019**, *9*, 9253–9258.
- [25] P. Gentili, S. Pedetti, *Chem. Commun.* **2012**, *48*, 5358–5360.
- [26] C. A. Brown, A. Yamashita, *J. Am. Chem. Soc.* **1975**, *97*, 891–892.
- [27] J. W. Amoroso, L. S. Borketey, G. Prasad, N. A. Schnarr, *Org. Lett.* **2010**, *12*, 2330–2333.
- [28] N. Pantalon Juraj, M. Krklec, T. Novosel, B. Perić, R. Vianello, S. Raić-Malić, S. I. Kirin, *Dalt. Trans.* **2020**, *49*, 9002–9015.
- [29] G. G. Kleinspehn, J. A. Jung, S. A. Studniarz, *J. Org. Chem.* **1967**, *32*, 460–462.
- [30] M. Vashishtha, M. Mishra, D. O. Shah, *Green Chem.* **2016**, *18*, 1339–1354.
- [31] T.-Y. Luo, C. Liu, S. V. Eliseeva, P. F. Muldoon, S. Petoud, N. L. Rosi, *J. Am. Chem. Soc.* **2017**, *139*, 9333–9340.
- [32] Y. Ji, D. A. DiRocco, C. M. Hong, M. K. Wismer, M. Reibarkh, *Org. Lett.* **2018**, *20*, 2156–2159.
- [33] G. A. Molander, J. A. C. Romero, *Tetrahedron* **2005**, *61*, 2631–2643.
- [34] W. S. Horne, C. D. Stout, M. R. Ghadiri, *J. Am. Chem. Soc.* **2003**, *125*, 9372–9376.

Entry for the Table of Contents



The 2-(hydroxyimino)aldehyde (HIA) group undergoes Norrish-Yang photoisomerization to cyclobutanol oxime and is under investigation as metal ions ligand. Here we use click chemistry as a straightforward procedure to obtain HIA-based functional molecules, we characterize the products obtained by UV irradiation with a LED source ($\lambda = 365$ nm) and we show by UV-Vis spectrometry that HIAs specifically interact with Cu(II).